Chirality Dependent Charge Transfer Rate in Oligopeptides

Chirality Dependent Charge Transfer Rate in Oligopeptides.

Francesco Tassinari[1], Dilhara R. Jayarathna[2], Nirit Kantor-Uriel[1], Kathryn L. Davis[3], Vaibhav Varade[1], Catalina Achim[2], Ron Naaman[1]

[1]Department of Chemical and Biological Physics, Weizmann Institute of Science, Rehovot, 76100 Israel
[2]Department of Chemistry, Carnegie Mellon University, Pittsburgh, 15213 PA, USA
[3]Department of Chemistry, Manchester University, North Manchester, 46962 IN, USA

Abstract

It is shown that "spontaneous magnetization" occurs when chiral oligopeptides are attached to ferrocene and are self-assembled on a gold substrate. As a result, the electron transfer, measured by electrochemistry, shows asymmetry in the redox and oxidation rate constants and this asymmetry is reversed between the two enantiomers. The results are explained by the chiral induced spin selectivity of the electron transfer. The magnetization measured shows high anisotropy and the "easy axis" is along the molecular axis.

Keywords: electron transfer, self-assembled monolayers, magnetization, chirality, spin.

Introduction

Bio-molecules and among them oligopeptides and proteins are suggested as material for self-assembled electronic and sensing devices.[1,2] Specifically, self-assembled organic monolayers on gold are a very popular tool for studying charge transfer through molecules.[3,4,5] Typically the system includes a redox group attached to the tail of the adsorbed molecules of interest. The charge transfer between this group and the substrate is monitored either optically, using lasers,[6] or by electrochemistry.[7] It is almost natural to assume that the gold substrate and the redox group do not change their properties upon assembly. However, past experiments indicated that the simple description of gold surface, bridge organic molecule, and redox group as independent components is not complete and new properties may emerge when these three components are connected. For example, several groups reported that gold may show magnetic properties when molecules are self-assembled on its surface.[8-13] The magnetic properties were explained as resulting from both Pauli and orbital paramagnetism in the gold.[14] Furthermore, spin-dependent electron transfer was found when a monolayer of organic molecules containing paramagnetic atoms was adsorbed on gold, which indicates that the gold is magnetized.[15] The magnetic properties of gold may influence electron transfer through self-assembled monolayer of chiral molecules: in recent years it was established that electron transfer through chiral systems is spin dependent.[16] If the gold is indeed magnetic, its direction of magnetization may affect the spin of the electrons or holes injected from the substrate into the chiral molecule and thereby affect the charge transfer rate through the chiral molecule. In the present study, we investigated electrochemically the charge transfer through a self-assembled monolayer of chiral oligopeptides with a terminal ferrocene group adsorbed on the gold substrate.

Several groups have reported an asymmetry in the charge transfer through short oligopeptides, which contain L-aminoacids and adopt an α-helix structure. The rate constant for charge transfer from the electrode to the redox active group, situated at the opposite end of the molecule, is higher than the rate constant for transfer in the opposite sense.[17,18] This experimental observation was attributed to the relative orientation of the electrostatic field in the self-assembled monolayer (SAM), generated by the dipole moment of the oligopeptide itself , with respect to the direction in which the charge carriers propagate. The electrostatic field generated by the dipole moment of the molecule is largely due to the close packing and parallel orientation of the molecules in the monolayer.[19]

While we were studying the rate constant for charge transfer through L- and D-oligopeptide monolayers by electrochemistry, we observed that the asymmetry in the charge transfer rate is opposite for the two enantiomers. Since the orientation of the dipole moment inside the monolayer is the same for the two enantiomers, the asymmetry cannot be related to the dipole moment orientation. We propose an explanation of the observed asymmetry based on the chiral induced spin selectivity (CISS) effect in the electron transfer[20] and the magnetization of the gold substrate.

Materials and Methods

Peptide synthesis

The sequence of the peptides was designed with the goal that the peptides (1) are as short as possible to make the synthesis simple and (2) adopt a helical structure. The D/L-12-mer peptides Cya-(D/L-ala)$_3$-aib-(D/L-ala)$_2$-aib-(D/L-ala)$_2$-aib-(D/L-ala)$_2$ satisfy these requirements.[21,22] The incorporation of 2-amino isobutyric acid into the sequence of the peptides makes more hydrophilic and quite soluble when compared to, for example, polyalanine. This in turn made the purification of the peptides by reverse phase HPLC relatively simple. D/L-12-mer–Fc [Cya-(D/L-ala)$_3$-aib-(D/L-ala)$_2$-aib-(D/L-ala)$_2$-aib-(D/L-ala)$_2$-Ferrocene] peptides (cya = cysteamine; ala = alanine; aib = aminoisobutyric acid) were synthesized manually using Fmoc-solid phase peptide synthesis strategy, starting form commercially available Cysteamine-4-methoxytrityl resin with a loading of ~0.83 meq/g (Anaspec). Fmoc-D/L-alanine(ala)-OH (Anaspec) was coupled using 1-[Bis(dimethylamino)methylene]-1H-1,2,3-triazolo[4,5-b]pyridinium 3-oxid hexafluorophosphate (HATU, Chem-Impex) as coupling reagent. 6-Chloro-benzotriazole-1-yloxy-tris-pyrrolidinophosphonium hexafluoro-phosphate (PyClock: Peptides International) was used as the coupling of Fmoc-2-aminoisobutyric acid (aib)-OH (Anaspec). 2-(1*H*-benzotriazol-1-yl)-1,1,3,3-tetramethyluronium hexafluorophosphate (HBTU: Chem-Impex) was used as the coupling reagent for Ferrocene carboxylic acid (Sigma Aldrich). Anhydrous N,N'-Diisopropylethylamine and anhydrous N-Methyl-2-pyrrolidone (Sigma Aldrich) were used as the base and the solvent, respectively. The success of coupling each amino acid was monitored by qualitative Kaiser test. The peptides were cleaved from the resin with a cleavage cocktail of 95% Trifluoroacetic acid (EMD), 2.5% Triisopropylsilane (Sigma Aldrich), 2.5% water and two drops of immobilized tris(2-carboxyethyl)phosphine disulfide reducing gel (Thermo Scientific). Crude peptides were precipitated with cold diethyl ether (EMD) and dried

under nitrogen. Peptides were purified by reversed-phase high pressure liquid chromatography (HPLC) using a C18 silica column on a Waters 600 controller and pump. Absorbance was monitored with a Waters 2996 photodiode array detector. The peptides have been characterized by Electron Spray Ionization-Mass Spectroscopy (ESI-MS). Calc/exp: D-12-mer-Fc 1184.2/1184.2 and L-12-mer-Fc 1184.2/1184.2 (see Figure S1). Samples of the lyophilized D/L-12-mer-Fc were dissolved a 1:1 (v/v) mixtue of 2,2,2-trifluoroethanol (TFE) and nano pure water.

CD Spectroscopy

The CD spectra for the peptides were measured in 1:1 (v/v) mixture of 10 mM, pH 7.00 sodium phosphate buffer and TFE, in 0.1-cm path length cuvettes, at 20^{o}C on a JASCO J-715 spectrometer equipped with a thermoelectrically controlled single-cell holder. The scan rate was 100 nm/min and 10 scans were accumulated for each spectrum. The concentration of the peptides was 0.1 mg/ml. The helix content of the peptides was determined from the CD data using the equations:[23]

$$f_H = -([\theta]_{222} + 2340)/30300$$

where $[\theta]_{222}$ is the mean residue ellipticity at 222 nm, and f_H is the fraction of helix (both α and 3_{10}).

$$[\theta]_{222}(\deg cm^2\ dmol^{-1}) = \theta_{222} \times M/[10 \times d \times C \times (N-1)]$$

where θ_{222} is the observed ellipticity in degrees at 222 nm, M is the molecular weight of the peptide, d is the path length in cm, C is the concentration in g/ml, and N is the number of peptide bonds in the peptide[24].

Table 1: θ_{222} nm/θ_{208} nm and f_H percentage helix content of the peptides

Peptide	θ_{222} nm/θ_{208} nm	f_H
D-12 mer Fc	0.75±0.02	32±1
L-12 mer Fc	0.71±0.02	33±1

Monolayer formation

For the samples used in the electrochemistry experiments and the characterizations, the 120-nm thick gold surfaces were prepared by e-beam evaporation on a p-doped silicon wafer, using 3nm of chromium as the adhesion layer. For the samples used in the SQUID measurements, 8nm of titanium instead of 3nm of chromium were used as the adhesion layer, to avoid the complications

to the measurements arising from the magnetic properties of chromium. For the samples used in the magnetic AFM measurements (m-AFM), the surfaces were prepared by sputtering 120nm of nickel, followed by a 8nm thick gold layer on top of a silicon wafer with a 2μm thermal silicon oxide layer, with a 8nm titanium as the adhesion layer. The use of the Ni/Au surfaces for the mAFM measurements was necessary in order to be able to spin-polarize the electrons injected from the surface using an external magnetic field. All the surfaces were cleaned by boiling them first in acetone and then in ethanol for 10 minutes, followed by a UV-ozone cleaning for 15 minutes and a final incubation in warm ethanol for 40 minutes.

The surfaces, dried with a nitrogen gun, where immediately immersed into the peptide solution (0.625mg/mL, using a 1:1 mixture of NaPi 10mM pH=7 and TFE as solvent) and incubated for 36 h. After the incubation, the surfaces were rinsed 3 times with deionized water, dried with a nitrogen gun and immediately used for the experiments. The monolayers were characterized by AFM measurements (see supplementary information) as well as by IR spectroscopy,contact potential difference (CPD) studies, SQUID measurements and cyclic voltammetries.

PM-IRRAS

Infrared spectra were recorded in polarization modulation–infrared reflection–absorption mode (PM–IRRAS), using a Nicolet 6700 FTIR instrument, equipped with a PEM-90 photoelastic modulator (Hinds Instruments, Hillsboro, OR), at an 80° angle of incidence. The orientation of the peptides on the gold surface was determined using the following equation[25]:

$$\frac{I_1}{I_2} = 1.5 \times \left[\frac{(3\cos^2\gamma - 1)(3\cos^2\theta_1 - 1) + 2}{(3\cos^2\gamma - 1)(3\cos^2\theta_2 - 1) + 2}\right]$$

where I_1 and I_2 are the intensity of the amide I and amide II bands, θ_1 and θ_2 are the angles between the transition moment of the two bonds and the helical axis (which were found in the literature to be 39^o and 75^o respectively[26]) and γ is the tilt angle of the helix in respect to the surface normal.

Electrochemistry

The electrochemical experiments consisted in cyclic voltammetry experiments carried out at different scan rates (*v*) ranging from 10mV/s to 100mV/s in a potential window from 0.0 to 0.7V, using the oligopeptide modified gold surface as working electrode.
The measurements were done using a standard three-electrode setup, in a supporting electrolyte

solution of 0.1M $NaClO_4$, using a Pt wire as the counter electrode and an Ag/AgCl (sat. KCl) electrode as reference,The instrument used was an Autolab PGSTAT 20 potentiostat. Following the same approach used by Waldeck and collaborators[27], the charge transfer rate constant k^0 was obtained from the experimental data by plotting the anodic and cathodic peak separation (E_p-E_0) versus the normalized scan rate (v/k^0) and fitting the data by a curve obtained by Marcus theory, using a recombination energy (λ) of 0.8eV for the ferrocene.

The surface coverage Γ is calculated integrating the charge under the faradaic current peaks at a scan rate of 50mV/s.

Contact Potential Difference

Table 2: Contact potential difference (CPD) of gold coated with SAM of oligopeptides

	CPD (V)
Gold (blank)	0.0 ±0.004
L-12mer-Fc monolayer	-0.539 ±0.017
D-12mer-Fc monolayer	-0.486 ±0.006

The Contact Potential Difference (CPD) of the surfaces was determined using a commercial Kelvin probe instrument (Delta Phi Besocke, Jülich, Germany) within a Faraday cage. The reference probe consisted of a gold grid. The measurements were held in the dark and in ambient atmosphere. The CPD signal of a blank gold substrate was taken as the zero value. The CPD of the monolayers is reported as the difference between the gold reference and the value recorded for the monolayers after letting the signal stabilize. The results are summarized in Table 2.

SQUID measurements

The magnetic properties were measured using a SQUID (superconducting quantum interference device) magnetometer MPMS3 (L.O.T.- Quantum Design inc.) with the magnetic field applied either parallel or perpendicular to the sample plane. The vibrating sample magnetometry (VSM) were in use. The measurements were conducted at 300K, and consisted in a magnetizing run from 0Oe to 5000Oe, a first measurement going from 5000Oe to -5000Oe, a second going from -5000Oe to 5000Oe, and a demagnetizing run from 5000Oe to 0Oe. The diamagnetic contribution of the gold-titanium-silicon substrate was measured prior to the monolayer formation and subtracted from the final data.

Results and Discussion

We have studied by electrochemistry SAM of D/L-12mer-Fc peptides. The cysteamine (Cya) situated at the C-end of the peptide was used for covalent binding to the gold electrode. The ferrocene (Fc) situated at the N-end of the peptide plays the role of electron donor or acceptor depending on the potential applied to the gold electrode. The circular dichroism (CD) spectra of a solution of the L-peptide shows negative peaks at 208 nm and 222 nm and a positive peak at 192 nm, which are characteristic of a right-handed helix, while the D-peptide spectra, having a left-handed helix, shows opposite peaks (Figure 1a). The θ_{222} nm/θ_{208} nm values reported in Table 1 are indicative of both L- and D- peptides adopting a mixed $3_{10}/\alpha$ helical structure in solution.[19]

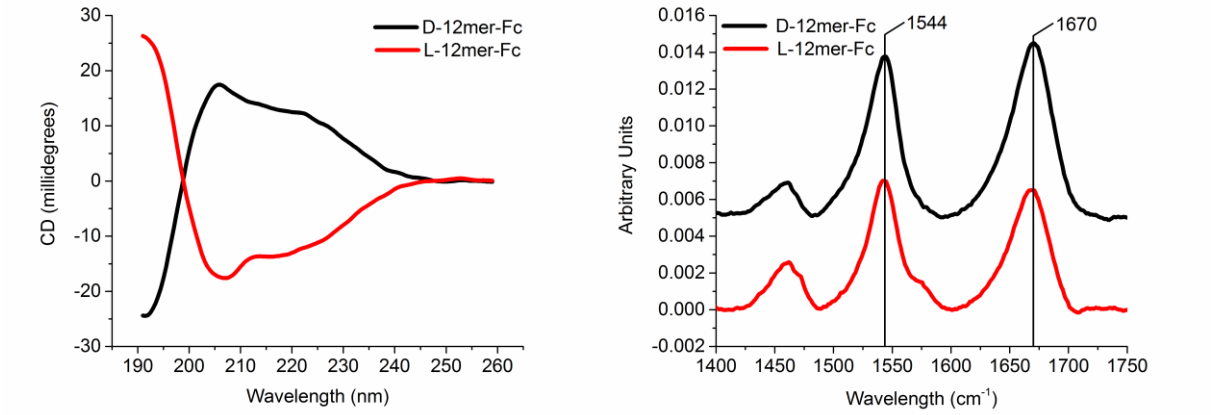

Figure 1: (a) CD spectra for 0.1 mg/ml solutions of the D/L-12 mer-Fc in 1:1 (v/v) TFE : pH 7.00 10 mM sodium phosphate buffer.; (b) The amide region of PMIRRAS spectra recorded for the self-assembled monolayers of L-12mer-Fc and D-12mer-Fc. The D-12mer-Fc spectra is shifted up for clarity.

The PM-IRRAS spectra of the adsorbed L- and D- peptides are identical in terms of both the position and the relative intensity of the amide I and II absorption bands, observed at 1670 cm^{-1} and 1544 cm^{-1}, respectively (Figure 1b). These bands are similar to the ones previously observed for SAMs of poly-L-alanine (1658 cm^{-1} and 1545 cm^{-1})[28] and indicate that the two peptides adopt a α-helix structure in the self-assembled monolayer. The analysis of the electrochemistry data prove that the self-assembled monolayers of D/L-12mer-Fc peptides, formed on gold, have similar surface coverage (Table 3). The extracted tilt angle, γ, of the helix

with respect to the surface normal is 48°, which is in good agreement to the reported value for similar systems.[16] Hence, the properties determined using PM-IRRAS and surface coverage indicate that the two peptide enantiomers form similar monolayers and adopt the same structure within these monolayers.

Table 3. The electron transfer rate constants and surface coverage for the self-assembled monolayers of L/D-12mer-Fc

	Surface Coverage (mol/cm^2)	Rate constant Oxidation (s^{-1})	Rate constant Reduction (s^{-1})
L-12mer-Fc	$3.6*10^{-11}$	0.30±0.02	0.47±0.03
D-12mer-Fc	$3.7*10^{-11}$	0.48±0.03	0.28±0.03

The calculated electron transfer rate constants for the D and L peptides (Table 3) are close to what previously reported for a polyalanine 14-mer.[16] Figure 2 presents the experimental data compared to the theoretical curve for a k_0 of $0.48s^{-1}$. For the D-peptide, the rate constant, as determined by the analysis of the anodic process, is larger than that determined by the analysis of the cathodic process. In contrast, for the L-peptide, the situation is reversed and the rate constant determined from the cathodic process is larger than that determined from the anodic process.

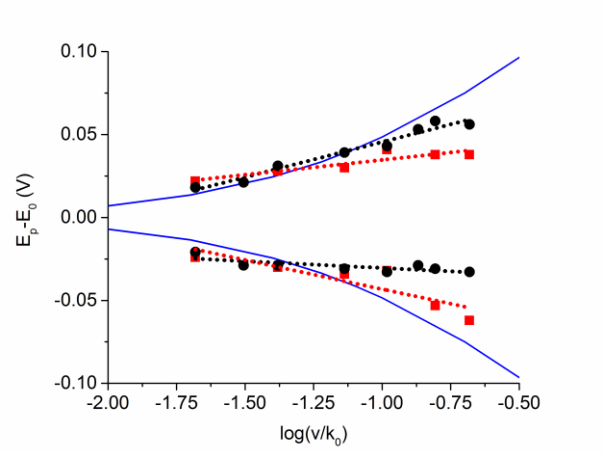

Figure 2. Plot of peak position relative to the formal potential (E_p-E_0) as a function of the normalized scan rate (v/k_0) for either L-12mer-Fc (red squares) or D-12mer-Fc (black dots). The blue solid lines are calculated using the Marcus theory applying a standard electrochemical rate constant (k_0) of 0.48 s^{-1} and assuming the reorganization energy for the ferrocene to be 0.8 eV. The dotted lines are a guide for the eye.

Several reasons have been suggested for the asymmetry in the rate constant for electron transfer through peptide monolayers, measured from the anodic and cathodic process: *1)* The

dipole moment of the helix was suggested to play a role, as it may favour electron-transfer in the direction towards the positive end of the dipole;[16] *2)* The amide-ferrocene strong electronic coupling promotes fast electron transfer[29] that would promote electron transfer between the C-terminal amide group and the sulphur, which was being considered the rate-determining step; *3)* the polarity of the Au-S junction defines a favourite direction for electron transfer.[17] These explanations cannot be used to rationalize the asymmetry observed for the two enantiomers because the orientation and strength of the dipole moment, the amide-ferrocene electronic coupling, and the polarity of the Au-S junction do not depend on the chirality of the two peptides. This is also supported by the CPD measurements reported in Table 2, showing that the change of the work function of the Au surfaces, after the monolayer formation, is similar for the two enantiomers.

The model we propose to explain the observed asymmetry in the rate constant for the two peptides is based on two components, the magnetization of the system and the spin selective electron transfer through the chiral molecules. It was reported before that linking chromophores to a substrate via organic monolayer may cause a large magnetic anisotropy in the sample.[30] Several groups already observed that binding paramagnetic molecules to gold, through an organic linker, causes spin selective conduction through the molecules.[15,31-33] Hence we propose, that as a result of the induced anisotropy, both the surface magnetization of the gold and the spin on the ferrocene are magnetized parallel to each other, along the axis of the molecule.

To verify this assumption, we measured the magnetization of the oligopeptide monolayer on gold at room temperature, using a superconducting quantum interference device (SQUID). Figure 3 shows the magnetic moment as a function of the magnetic field applied either perpendicular or parallel to the surface. The results are presented after the subtraction of the contribution of the substrate without the monolayer. A ferromagnetic response with a significant hysteresis is observed for both magnetic field directions. However, the response is non-isotropic. For the field applied perpendicular to the surface, the magnetic susceptibility is large and the hysteresis is about 40 Oe. For the magnetic field applied parallel to the surface, the magnetic susceptibility is somewhat smaller however the hysteresis is much larger, namely 120 Oe. Assuming that the measured magnetic moment at H=0 is proportional to the density of the monolayer, we calculated that per molecule the magnetic field corresponds to a 0.86 μ_B for the parallel field and 0.64 μ_B for the perpendicular one. These two values are consistent with a SAM

in which the molecules are at a tilt angle with respect to the surface normal of ~50°, which is similar to the tilt angle inferred from the PM IRRAS (48°). Based on these results, we conclude that the easy axis of the ferromagnet is along the molecular axis.

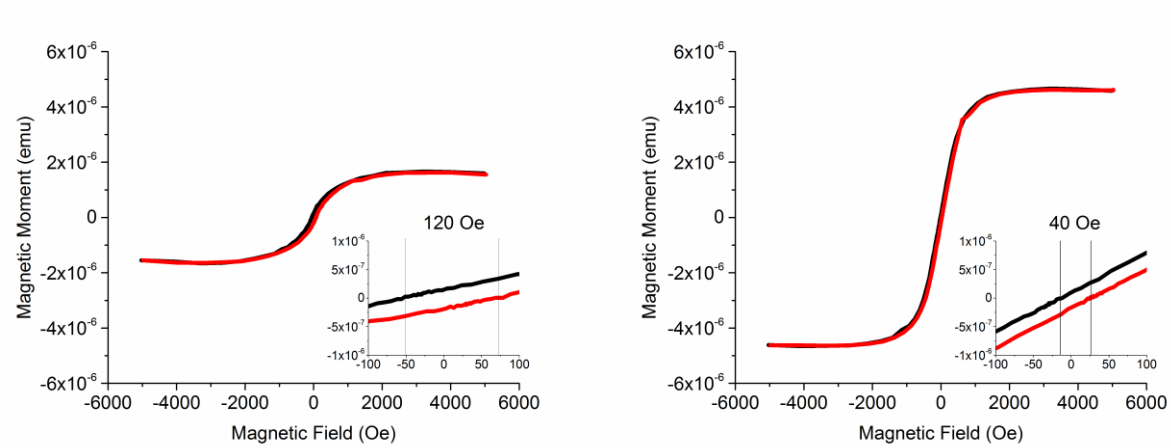

Figure 3: Magnetic moment versus magnetic field measured by SQUID at 300K for the L-12mer-Fc monolayer adsorbed on gold film. The substrate contribution to the signal has been subtracted from the data. The magnetic field was applied either parallel (a) or perpendicular (b) to the sample surface. The inset is a zoom of the low field region where the hysteresis is largest**.** Identical results were obtained for the D-12mer-Fc monolayer (see supplementary information).

In attempting to rationalize the enantio-dependant asymmetry in the electron transfer rate we propose a model that invokes spin-dependent electron transfer through the chiral molecules, an effect known as chiral-induced spin selectivity (CISS).[16] The CISS has inherent asymmetry, for a given enantiomer, the preferred spin of electrons conducted in one direction is the opposite to that of electrons conducted in the opposite direction. In our system, we assume that both the gold substrate and the ferrocene have a magnetic moment parallel to each other and to the molecular axis (see Figure 4).

The electrons injected into the oligopeptide have therefore their spin oriented in the same direction, independent if they are transferred from the gold or from the ferrocene and independent on the specific enantiomer. However, because of the CISS effect, in the case of the L-peptide the spin is oriented so that its transport is favoured for the reduction direction, while for the D-peptide it is favoured for the oxidation direction.

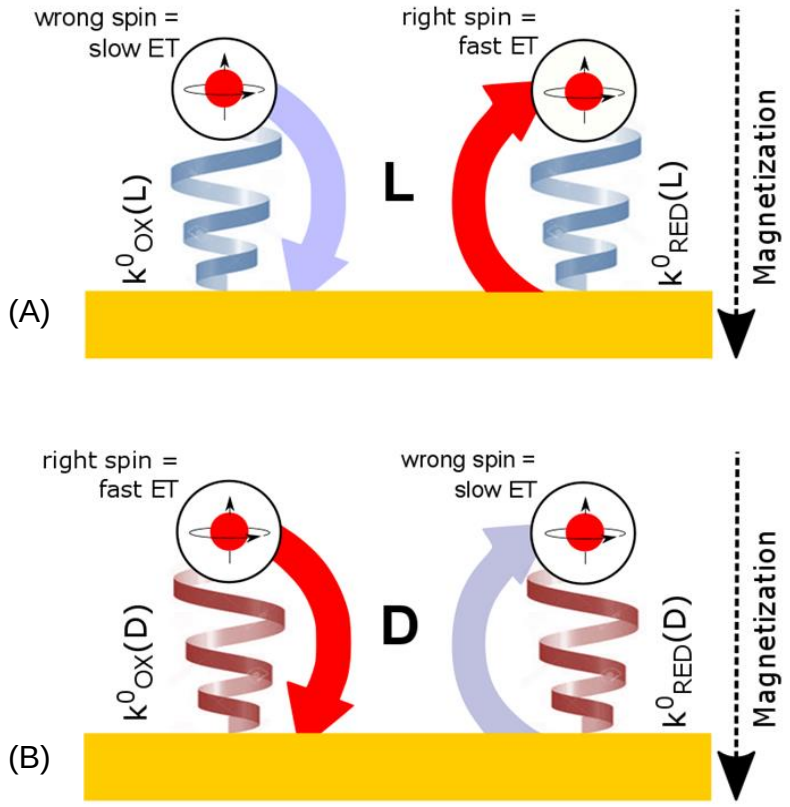

Figure 4: A scheme of the proposed mechanism for the asymmetric electron transfer. The gold is magnetized and as a result, one spin is injected preferentially from it to the molecule or vice versa. A) In the case of L-oligopeptide (right handed helix) the electron injected from the gold has a spin aligned parallel to the electron's velocity, which is the preferred spin for the electron transfer. As a result the electron transfer in this direction (reduction process) is faster than backwards. B) In the case of D-oligopeptide (left handed helix), the preferred spin orientation is when the spin is aligned antiparallel to the electron's velocity and therefore the preferred rate is for the oxidation process.

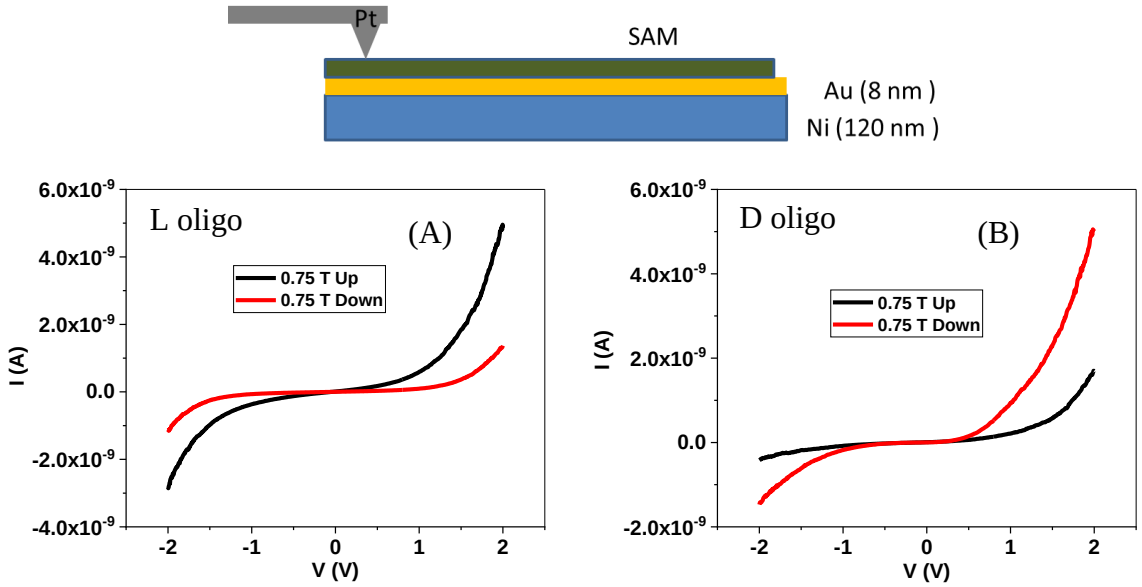

Figure 5: Spin dependent conduction through monolayers made from L-12mer-Fc or D-12mer-Fc molecules. The system is presented schematically in the upper scheme. The current versus voltage is presented for the L and D oligomers (A) and (B) respectively. While for the L enantiomer the current is higher when the Ni magnet is pointing up, for the D enantiomer it is higher for the magnet pointing down.

To verify the model suggested above, we performed spin dependent conduction studies using magnetic substrate and conducting AFM tip. The current versus voltage was measured on the monolayer with the magnetic field applied to the Ni substrate applied perpendicular to the surface and pointing up or down with respect to the surface. The potential is that of the Pt tip. The results shown in Figure 5 indicate that the current through the monolayer depends strongly (typically by a factor of 4) on the direction of the magnetic field (typically a ratio of 4:1, and implicitly on the spin orientation. It is also clear that when the magnetic field is pointing up, the reduction (positive voltage) is favoured over oxidation (negative voltage) for the L enantiomer, while when the field is pointing down, the oxidation is favoured for the D enantiomer. Thus the spin dependent transport studies corroborate the importance of spontaneous magnetization of the system as well as the spin selectivity in the electron transfer.

This work is an example for “spontaneous magnetization” that affects the charge transfer rates in chiral molecules. The observations presented here are consistent with the asymmetry in

electron transfer observed in former studies.[17,18] However, because of our ability to probe both enantiomers the mechanism for the process was revealed. Since in Nature paramagnetic ions are abundant in proteins and since proteins are chiral, similar effects may be relevant also in biological systems.

Acknowledgements

RN acknowledges the support from the Israel Science Foundation and by the European Research Council under the European Union's Seventh Framework Program (FP7/2007-2013)/ERC grant agreement n° 338720 CISS and by the Templeton Foundation. CA acknowledges financial support from the US NSF (CHE-1413202) and interesting discussions with Dr. Yossi Paltiel. The authors acknowledge the help of Dr. Gregory Leitus with the measurements of the magnetic properties of the samples and Dr. Davide Ceratti for helpful discussions.

References

[1] A. B. Marciel, M. Tanyeri, B. D. Wall, J. D. Tovar, C. M. Schroeder, W. L. Wilson, *Adv. Mater*. **2013**, *25*, 6398.

[2] J. I. N. Oliveira, E.L. Albuquerque, U.L. Fulco, P.W. Mauriz, R.G. Sarmento, *Chem. Phys. Lett.* **2014,** *612*, 14.

[3] C. E. D. Chidsey, *Science* **1991,** *251*, 919.

[4] M. M. Galka, H. B. Kraatz, *ChemPhysChem* **2002**, *3*, 356.

[5] M. Kettner, B. Göhler, H. Zacharias, D. Mishra, V. Kiran, R. Naaman,C. Fontanesi, D. H. Waldeck,S. Sęk, J. Pawłowski, J. Juhaniewicz, *J. Phys. Chem. C* **2015**, *119*, 14542.

[6] H. S. Kato Y. Murakami, Y. Kiriyama, R. Saitoh, T. Ueba, T.Yamada, Y. Ie, Y. Aso, T. Munakata, *J. Phys. Chem. C* **2015**, *119***,** 7400.

[7] A. L. Eckermann, D. J. Feld, J. A. Shaw, T. J. Meade, *Coord. Chem. Rev.* **2010**, *254*, 1769.

[8] I. Carmeli, G. Leitus, R. Naaman, S. Reich, Z. Vager, *J. Chem. Phys.* **2003**, *118*, 10372.

[9] P. Crespo, R. Litrán, T. C. Rojas, M. Multigner, J. M. de la Fuente, J. C. Sánchez-López, M. A. García, A. Hernando, S. Penadés, and A. Fernández, *Phys. Rev. Lett.* **2004**, *93*, 087204.

[10] S. Trudel, *Gold Bull.* **2011**, *44*, 3.

[11] R. Singh, *J. Magn. Magn. Mater.* **2013**, *346*, 58.

[12] G. L. Nealon, B. Donnio, R. Greget, J. P. Kappler, E. Terazzi, J. L. Gallani, *Nanoscale* **2012**, *4*, 5244.

[13] M. Agrachev, S. Antonello, T. Dainese, M. Ruzzi, A. Zoleo, E. Aprà, N. Govind, A. Fortunelli, L. Sementa, F. Maran, *ACS Omega* **2017**, *2*, 2607.

[14] M. Suzuki, N. Kawamura, H. Miyagawa, J. S. Garitaonandia, Y. Yamamoto, H. Hori, *Phys. Rev. Lett.* **2012**, *108*, 047201.

[15] A. C. Aragonès, D. Aravena, J.I. Cerdá, Z. Acís-Castillo, H. Li, J.A. Real, F. Sanz, J. Hihath, E. Ruiz, I. Díez-Pérez, *Nano Lett.* **2016**, *16*, 218.

[16] R. Naaman, D. H. Waldeck, *Ann. Rev. Phys. Chem.* **2015**, *66*, 263.

[17] S. Sek, A. Tolak, A. Misicka, B. Palys, R. Bilewicz, *J. Phys. Chem. B* **2005**, *109***,** 18433.

[18] M. Venanzi, E. Gatto, M. Caruso, A. Porchetta, F. Formaggio, C. Toniolo, *J. Phys. Chem. A* **2014**, *118***,** 6674.

[19] V.S. Lvov, R. Naaman, Z. Vager, V. Tiberkevich, *Chem. Phys. Lett.* **2003**, *381*, 650.

[20] K. Michaeli, N. Kantor-Uriel, R. Naaman, D. H. Waldeck, *Chem. Soc. Rev.* **2016**, *45*, 6478.

[21] C. Tonlolo, E. Benedetti, *Trends Biochem. Sci.*, **1991**, *16*, 350.

[22] S. Bezer, M. Matsumoto, M. W. Lodewyk, S. J. Lee, D. J. Tantillo, M. R. Gagné, M. L. Waters, , *Org. Biomol. Chem.*, **2014**, *12*), 1488.

[23] Y. H. Chen, J. T. Yang, H. M. Martinez, *Biochemistry* **1972**, *11*, 4120.

[24] C. Toniolo, A. Polese, F. Formaggio, M. Crisma, J. Kamphuis, *J. Am. Chem. Soc.* **1996,** *118*, 2744.

[25] D. E. López-Pérez, G. Revilla-López, D. Jacquemin, D. Zanuy, B. Palys, S. Sek, C. Alemán, *Phys. Chem. Chem. Phys.* **2012**, *14***,** 10332.

[26] Y. Miura, S. Kimura, Y. Imanishi, J. Umemura, *Langmuir* **1998**, *14***,** 6935.

[27] E. Wierzbinski, A. de Leon, K. L. Davis, S. Bezer, M. A. Wolak, M. J. Kofke, R. Schlaf, C. Achim, D. H. Waldeck, *Langmuir* **2012**, *28***,** 1971.

[28] S. Krimm, J. Bandekar, *Adv. Protein Chem.* **1986,** *38***,** 181.

[29] J. Watanabe, T. Morita, S. Kimura, *J. Phys. Chem. B* **2005,** *109***,** 14416.

[30] A. Zakrassov, A. Bitler, L. Etgar, G. Leitus, E. Lifshitz, R. Naaman, *Phys. Chem. Chem. Phys.* **2009**, *11*, 7549.

[31] A. Hernando, P. Crespo, M. A. Garcıá, *Phys. Rev. Lett.* **2006**, *96*, 057206.

[32] J. M. D. Coey, M. Venkatesan, C. B. Fitzgerald, A. P. Douvalis, I. S. Sanders, *Nature* **2002**, *420*, 156.

[33] T. L. Makarova, *Semiconductors* **2004**, *38*, 615.